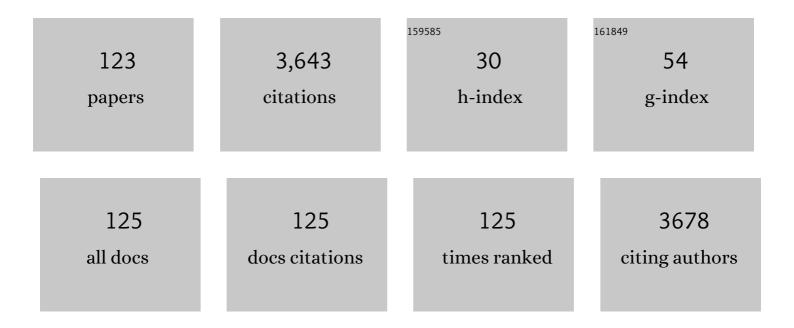
List of Publications by Year in descending order

Source: https://exaly.com/author-pdf/9521515/publications.pdf Version: 2024-02-01



Ελρίο Δεμτλρ

#	Article	IF	CITATIONS
1	A scalable metal-organic framework as a durable physisorbent for carbon dioxide capture. Science, 2021, 374, 1464-1469.	12.6	308
2	Structuring adsorbents and catalysts by processing of porous powders. Journal of the European Ceramic Society, 2014, 34, 1643-1666.	5.7	264
3	Microstructure, mechanical properties, electrical conductivity and wear behavior of high volume TiC reinforced Cu-matrix composites. Materials Characterization, 2009, 60, 327-336.	4.4	147
4	Strong and binder free structured zeolite sorbents with very high CO2-over-N2 selectivities and high capacities to adsorb CO2 rapidly. Energy and Environmental Science, 2012, 5, 7664.	30.8	144
5	Microstructure evolution and wear properties of in situ synthesized TiB2 and TiC reinforced steel matrix composites. Journal of Alloys and Compounds, 2008, 459, 491-497.	5.5	137
6	A study of the sintering of diatomaceous earth to produce porous ceramic monoliths with bimodal porosity and high strength. Powder Technology, 2010, 201, 253-257.	4.2	98
7	Mechanical Properties of a Metal–Organic Framework formed by Covalent Cross-Linking of Metal–Organic Polyhedra. Journal of the American Chemical Society, 2019, 141, 1045-1053.	13.7	89
8	Studies on the adsorption of chromium(VI) onto 3-Mercaptopropionic acid coated superparamagnetic iron oxide nanoparticles. Journal of Colloid and Interface Science, 2014, 425, 36-43.	9.4	87
9	Microstructure, mechanical and fretting wear properties of TiC-stainless steel composites. Materials Characterization, 2008, 59, 84-90.	4.4	85
10	Tensile behavior change depending on the varying tungsten content of W–Ni–Fe alloys. International Journal of Refractory Metals and Hard Materials, 2007, 25, 380-385.	3.8	78
11	TiB2 and TiC stainless steel matrix composites. Materials Letters, 2007, 61, 189-191.	2.6	73
12	Hierarchically Porous Ceramics from Diatomite Powders by Pulsed Current Processing. Journal of the American Ceramic Society, 2009, 92, 338-343.	3.8	70
13	High temperature tribology of CuMoTaWV high entropy alloy. Wear, 2019, 426-427, 412-419.	3.1	68
14	Novel Fabrication and Enhanced Photocatalytic MB Degradation of Hierarchical Porous Monoliths of MoO3 Nanoplates. Scientific Reports, 2017, 7, 1845.	3.3	64
15	Synthesis and Mechanical Characterization of a CuMoTaWV High-Entropy Film by Magnetron Sputtering. ACS Applied Materials & amp; Interfaces, 2020, 12, 21070-21079.	8.0	62
16	Laminated Adsorbents with Very Rapid CO <sub>2</sub> Uptake by Freeze-Casting of Zeolites. ACS Applied Materials & Interfaces, 2013, 5, 2669-2676.	8.0	61
17	Colloidal processing and CO2 capture performance of sacrificially templated zeolite monoliths. Applied Energy, 2012, 97, 289-296.	10.1	55
18	Strong Hierarchically Porous Monoliths by Pulsed Current Processing of Zeolite Powder Assemblies. ACS Applied Materials & Interfaces, 2010, 2, 732-737.	8.0	52

#	Article	IF	CITATIONS
19	Mechanical performance and CO2 uptake of ion-exchanged zeolite A structured by freeze-casting. Journal of the European Ceramic Society, 2015, 35, 2607-2618.	5.7	51
20	Highly porous open cellular TiAl-based intermetallics fabricated by thermal explosion with space holder process. Intermetallics, 2016, 68, 95-100.	3.9	51
21	Colloidal Processing and Thermal Treatment of Binderless Hierarchically Porous Zeolite 13X Monoliths for CO2 Capture. Journal of the American Ceramic Society, 2011, 94, 92-98.	3.8	49
22	A high-entropy B <sub>4</sub> (HfMo <sub>2</sub> TaTi)C and SiC ceramic composite. Dalton Transactions, 2019, 48, 5161-5167.	3.3	47
23	On the processing, microstructure, mechanical and wear properties of cermet/stainless steel layer composites. Acta Materialia, 2007, 55, 1467-1477.	7.9	44
24	Nanocellulose–Zeolite Composite Films for Odor Elimination. ACS Applied Materials & Interfaces, 2015, 7, 14254-14262.	8.0	44
25	Ceramic reinforced high modulus steel composites: processing, microstructure and properties. Canadian Metallurgical Quarterly, 2014, 53, 253-263.	1.2	43
26	Fabrication and properties of freeze-cast mullite foams derived from coal-series kaolin. Ceramics International, 2016, 42, 12414-12421.	4.8	43
27	An investigation on the solid state sintering of mechanically alloyed nano-structured 90W–Ni–Fe tungsten heavy alloy. International Journal of Refractory Metals and Hard Materials, 2008, 26, 145-151.	3.8	39
28	Ultra-high strength martensitic 420 stainless steel with high ductility. Additive Manufacturing, 2019, 29, 100803.	3.0	39
29	Adherent and low friction nano-crystalline diamond film grown on titanium using microwave CVD plasma. Diamond and Related Materials, 2008, 17, 294-299.	3.9	35
30	Advanced Mechanical Strength in Post Heat Treated SLM 2507 at Room and High Temperature Promoted by Hard/Ductile Sigma Precipitates. Metals, 2019, 9, 199.	2.3	34
31	High temperature tribology and wear of selective laser melted (SLM) 316L stainless steel. Wear, 2020, 448-449, 203228.	3.1	34
32	Effect of WC particle size on the microstructure, mechanical properties and fracture behavior of WC–(W, Ti, Ta) C–6wt% Co cemented carbides. International Journal of Refractory Metals and Hard Materials, 2007, 25, 405-410.	3.8	32
33	Porous mullite thermal insulators from coal gangue fabricated by a starch-based foam gel-casting method. Journal of the Australian Ceramic Society, 2017, 53, 287-291.	1.9	31
34	Subgrain-controlled grain growth in the laser-melted 316 L promoting strength at high temperatures. Royal Society Open Science, 2018, 5, 172394.	2.4	31
35	Aluminium matrix tungsten aluminide and tungsten reinforced composites by solid-state diffusion mechanism. Scientific Reports, 2017, 7, 12391.	3.3	30
36	Microstructure and properties of Ti5Si3-based porous intermetallic compounds fabricated via combustion synthesis. Journal of Alloys and Compounds, 2014, 612, 337-342.	5.5	29

#	Article	IF	CITATIONS
37	Synthesis and characterization of nano-crystalline CVD diamond film on pure titanium using Ar/CH4/H2 gas mixture. Materials Letters, 2007, 61, 2139-2142.	2.6	28
38	Oxidation properties of self-propagating high temperature synthesized niobium disilicide. Corrosion Science, 2014, 85, 311-317.	6.6	28
39	Synthesis, microstructure and properties of MoSi 2 –5 vol%Al 2 O 3 composites. Ceramics International, 2014, 40, 16381-16387.	4.8	27
40	Synthesis and Properties of MoSi≺sub>2–MoB–SiC Ceramics. Journal of the American Ceramic Society, 2016, 99, 1147-1150.	3.8	27
41	Hierarchical porous TiAl3 intermetallics synthesized by thermal explosion with a leachable space-holder material. Materials Letters, 2016, 181, 261-264.	2.6	26
42	Processing and Characterization of Refractory Quaternary and Quinary High-Entropy Carbide Composite. Entropy, 2019, 21, 474.	2.2	26
43	Mixed anionic surfactant-templated mesoporous silica nanoparticles for fluorescence detection of Fe <sup>3+</sup> . Dalton Transactions, 2016, 45, 508-514.	3.3	25
44	Development of Si3N4/Al composite by pressureless melt infiltration. Transactions of Nonferrous Metals Society of China, 2006, 16, 629-632.	4.2	24
45	Hierarchically porous binder-free silicalite-1 discs: a novel support for all-zeolite membranes. Journal of Materials Chemistry, 2011, 21, 8822.	6.7	24
46	Methylcellulose-Directed Synthesis of Nanocrystalline Zeolite NaA with High CO2 Uptake. Materials, 2014, 7, 5507-5519.	2.9	24
47	A novel fabrication strategy for highly porous FeAl/Al2O3 composite by thermal explosion in vacuum. Vacuum, 2018, 149, 225-230.	3.5	24
48	Combustion synthesis of (Mo1â^'xCrx)Si2 (x=0.00–0.30) alloys in SHS mode. Advanced Powder Technology, 2012, 23, 133-138.	4.1	20
49	Preparation of graded silicalite-1 substrates for all-zeolite membranes with excellent CO 2 /H 2 separation performance. Journal of Membrane Science, 2015, 493, 206-211.	8.2	20
50	Aluminophosphate monoliths with high CO <sub>2</sub> -over-N <sub>2</sub> selectivity and CO <sub>2</sub> capture capacity. RSC Advances, 2014, 4, 55877-55883.	3.6	19
51	Effect of heating rate on porous TiAl-based intermetallics synthesized by thermal explosion. Materials and Manufacturing Processes, 2017, 32, 489-494.	4.7	19
52	Enhanced sintering, microstructure evolution and mechanical properties of 316L stainless steel with MoSi2 addition. Journal of Alloys and Compounds, 2011, 509, 8794-8797.	5.5	18
53	Microstructure Evolution and Pore Formation Mechanism of Porous TiAl3 Intermetallics via Reactive Sintering. Acta Metallurgica Sinica (English Letters), 2018, 31, 440-448.	2.9	18
54	Exothermic behavior and thermodynamic analysis for the formation of porous TiAl3 intermetallics sintering with different heating rates. Journal of Alloys and Compounds, 2019, 811, 152056.	5.5	18

#	Article	IF	CITATIONS
55	Mechanically activated reactive synthesis of refractory molybdenum and tungsten silicides. International Journal of Refractory Metals and Hard Materials, 2008, 26, 173-178.	3.8	17
56	Reactive sintering and properties of TiB2 and TiC porous cermets. Materials Letters, 2008, 62, 1242-1245.	2.6	17
57	Porous alumina ceramics by gel casting: Effect of type of sacrificial template on the properties. International Journal of Ceramic Engineering & Science, 2019, 1, 77-84.	1.2	17
58	Enhanced Mechanical, Thermal and Electrical Properties of Highâ€Entropy HfMoNbTaTiVWZr Thin Film Metallic Glass and its Nitrides. Advanced Engineering Materials, 2022, 24, .	3.5	16
59	High temperature tribology of polymer derived ceramic composite coatings. Scientific Reports, 2018, 8, 15105.	3.3	15
60	Effect of SiC on Microstructure, Phase Evolution, and Mechanical Properties of Spark-Plasma-Sintered High-Entropy Ceramic Composite. Ceramics, 2020, 3, 359-371.	2.6	15
61	Self-propagating high temperature synthesis of MoSi2 matrix composites. Rare Metals, 2006, 25, 225-230.	7.1	14
62	High Temperature Performance of Spark Plasma Sintered W0.5(TaTiVCr)0.5 Alloy. Metals, 2020, 10, 1512.	2.3	14
63	Tribological performance of Ti6Al4V at elevated temperatures fabricated by electron beam powder bed fusion. Tribology International, 2021, 153, 106658.	5.9	14
64	Microstructure and property evolution during the sintering of stainless steel alloy with Si3N4. Materials Science & Engineering A: Structural Materials: Properties, Microstructure and Processing, 2008, 472, 324-331.	5.6	13
65	Highly Structured Nanofiber Zeolite Materials for Biogas Upgrading. Energy Technology, 2020, 8, 1900781.	3.8	13
66	Freeze Granulated Zeolites X and A for Biogas Upgrading. Molecules, 2020, 25, 1378.	3.8	13
67	Preparation and highâ€ŧemperature oxidation resistance of multilayer MoSi <sub>2</sub> /MoB coating by spent MoSi <sub>2</sub> â€based materials. Journal of the American Ceramic Society, 2021, 104, 3682-3694.	3.8	13
68	Two-step growth of high-quality nano-diamond films using CH4/H2 gas mixture. Vacuum, 2007, 81, 713-717.	3.5	12
69	Structured emulsion-templated porous copolymer based on photopolymerization for carbon capture. Journal of CO2 Utilization, 2017, 21, 473-479.	6.8	12
70	Thin zeolite laminates for rapid and energy-efficient carbon capture. Scientific Reports, 2017, 7, 10988.	3.3	12
71	Optimized cesium and potassium ion-exchanged zeolites A and X granules for biogas upgrading. RSC Advances, 2018, 8, 37277-37285.	3.6	12
72	Fabrication and Characterization of Highly Porous FeAlâ€Based Intermetallics by Thermal Explosion Reaction. Advanced Engineering Materials, 2019, 21, 1801110.	3.5	12

#	Article	IF	CITATIONS
73	A phase conversion method to anchor ZIF-8 onto a PAN nanofiber surface for CO <sub>2</sub> capture. RSC Advances, 2021, 12, 664-670.	3.6	12
74	Processing of Macroporous Alumina Ceramics Using Pre-Expanded Polymer Microspheres as Sacrificial Template. Ceramics, 2018, 1, 329-342.	2.6	11
75	Processing, microstructure and high temperature dry sliding wear of a Cr-Fe-Hf-Mn-Ti-Ta-V high-entropy alloy based composite. Materials Today Communications, 2021, 28, 102657.	1.9	11
76	Preparation, properties and high-temperature oxidation resistance of MoSi2-HfO2 composite coating to protect niobium using spent MoSi2-based materials. Ceramics International, 2021, 47, 27091-27099.	4.8	11
77	Fabrication of MoSi2 coatings on molybdenum and its high-temperature anti-oxidation properties. Transactions of Nonferrous Metals Society of China, 2022, 32, 935-946.	4.2	11
78	Processing, microstructure, properties and wear behavior of in situ synthesized TiB2 and TiC thick films on steel substrates. Surface and Coatings Technology, 2007, 201, 9603-9609.	4.8	10
79	Synthesis, microstructure and mechanical properties of (Mo,Ti)Si2/Al2O3 composites prepared by thermite-reaction-assisted combustion synthesis. Journal of Alloys and Compounds, 2016, 688, 870-877.	5.5	10
80	Oxidation Resistance of Highly Porous Fe-Al Foams Prepared by Thermal Explosion. Metallurgical and Materials Transactions A: Physical Metallurgy and Materials Science, 2018, 49, 3683-3691.	2.2	10
81	TiC-maraging stainless steel composite: microstructure, mechanical and wear properties. Rare Metals, 2006, 25, 630-635.	7.1	9
82	Effect of Cu3P addition on sintering behaviour of elemental powders in the composition of 465 stainless steel. Powder Metallurgy, 2006, 49, 28-33.	1.7	9
83	Behavior of residual carbon in Sm(Co, Fe, Cu, Zr)z permanent magnets. Journal of Alloys and Compounds, 2007, 440, 89-93.	5.5	9
84	Effect of the composition of starting materials of Mo–Si on the mechanically induced self-propagating reaction. Journal of Alloys and Compounds, 2008, 456, 304-307.	5.5	9
85	Effects of tungsten and aluminum additions on the formation of molybdenum disilicide by mechanically-induced self-propagating reaction. Journal of Alloys and Compounds, 2010, 490, 388-392.	5.5	9
86	Effect of annealing environment on the crack healing and mechanical properties of (Mo0.97Nb0.03)(Si0.97Al0.03)2. Journal of Alloys and Compounds, 2015, 634, 109-114.	5.5	9
87	Transformation of metastable dual-phase (Ti0.25V0.25Zr0.25Hf0.25)B2 to stable high-entropy single-phase boride by thermal annealing. Applied Physics Letters, 2021, 119, .	3.3	9
88	Synthesis, microstructure and mechanical properties of Al2O3 reinforced Ni3Al matrix composite. Materials Science & Engineering A: Structural Materials: Properties, Microstructure and Processing, 2009, 499, 415-420.	5.6	8
89	Formation of Moâ^'Siâ^'Ti Alloys by Selfâ^'propagating Combustion Synthesis. Materials Research, 2015, 18, 806-812.	1.3	8
90	Laminated porous diatomite monoliths for adsorption of dyes from water. Environmental Progress and Sustainable Energy, 2019, 38, S377.	2.3	8

#	Article	IF	CITATIONS
91	Carbon-reinforced MgCl2 composites with high structural stability as robust ammonia carriers for selective catalytic reduction system. Journal of Environmental Chemical Engineering, 2020, 8, 103584.	6.7	8
92	Bibliometric Mapping of Literature on High-Entropy/Multicomponent Alloys and Systematic Review of Emerging Applications. Entropy, 2022, 24, 329.	2.2	8
93	Sintering behavior, microstructure and properties of TiC-FeCr hard alloy. International Journal of Minerals, Metallurgy, and Materials, 2007, 14, 89-93.	0.2	7
94	Effect of diluent on the synthesis of molybdenum disilicide by mechanically-induced self-propagating reaction. Journal of Alloys and Compounds, 2010, 494, 301-304.	5.5	7
95	Microsphere Assemblies via Phosphonate Monoester Coordination Chemistry. Chemistry - A European Journal, 2018, 24, 1533-1538.	3.3	7
96	Preparation of Porous NiAl Intermetallic with Controllable Shape and Pore Structure by Rapid Thermal Explosion with Space Holder. Metals and Materials International, 2021, 27, 4216-4224.	3.4	7
97	Effect of Additive Cu-10Sn Alloy on Sintering Behavior of Elemental Powders in Composition of 465 Stainless Steel. Journal of Iron and Steel Research International, 2007, 14, 61-64.	2.8	6
98	Sintering Behavior of Elemental Powders with FeB Addition in the Composition of Martensitic Stainless steel. Journal of Materials Engineering and Performance, 2007, 16, 726-729.	2.5	6
99	Solidâ€state <sup>13</sup> C, <sup>15</sup> N and <sup>29</sup> Si NMR characterization of block copolymers with CO <sub>2</sub> capture properties. Magnetic Resonance in Chemistry, 2016, 54, 734-739.	1.9	6
100	Surface microstructural changes of spark plasma sintered zirconia after grinding and annealing. Ceramics International, 2016, 42, 15610-15617.	4.8	6
101	Effect of 10Âwt% VC on the Friction and Sliding Wear of Spark Plasma–Sintered WC–12Âwt% Co Cemented Carbides. Tribology Transactions, 2017, 60, 276-283.	2.0	6
102	Fabrication of Highly Porous CuAl Intermetallic by Thermal Explosion Using NaCl Space Holder. Jom, 2018, 70, 2173-2178.	1.9	6
103	Recycling Molybdenum Oxides from Waste Molybdenum Disilicides: Oxidation Experimental Study and Photocatalytic Properties. Oxidation of Metals, 2019, 92, 1-12.	2.1	6
104	Porous Strontium Chloride Scaffolded by Graphene Networks as Ammonia Carriers. Advanced Functional Materials, 2021, 31, 2008505.	14.9	6
105	Refractory multicomponent boron-carbide high entropy oxidation-protective coating for carbon-carbon composites. Surface and Coatings Technology, 2021, 425, 127697.	4.8	6
106	Magnetic properties and microstructure of radially oriented Sm(Co,Fe,Cu,Zr)z ring magnets. Materials Letters, 2007, 61, 5271-5274.	2.6	5
107	A new kind of age hardenable martensitic stainless steel with high strength and toughness. Ironmaking and Steelmaking, 2007, 34, 285-289.	2.1	4
108	A new method to process high strength TiCN stainless steel matrix composites. Powder Metallurgy, 2007, 50, 250-254.	1.7	4

#	Article	IF	CITATIONS
109	Influence of heat treatment on fracture and magnetic properties of radially oriented Sm2Co17 permanent magnets. Transactions of Nonferrous Metals Society of China, 2007, 17, 491-495.	4.2	4
110	Solution-mediated growth of NBA-ZSM-5 crystals retarded by gel entrapment. Journal of Crystal Growth, 2018, 487, 57-64.	1.5	4
111	In situ fabrication and properties of 0.4MoB-0.1SiC-xMoSi2 composites by self-propagating synthesis and hot-press sintering. Ceramics International, 2018, 44, 51-56.	4.8	4
112	Microstructure-Tailored Stainless Steels with High Mechanical Performance at Elevated Temperature. , 2019, , .		4
113	Ab initio aided design of novel quaternary, quinary and senary high-entropy borocarbides. Journal of Materials Science, 2022, 57, 422-443.	3.7	4
114	Chemical durability of hierarchically porous silicalite-I membrane substrates in aqueous media. Journal of Materials Research, 2013, 28, 2253-2259.	2.6	3
115	Processing, microstructure and properties of hierarchically porous Cu. Materials Express, 2016, 6, 271-276.	0.5	3
116	Rapid Ammonia Carriers for SCR Systems Using MOFs [M2(adc)2(dabco)] (M = Co, Ni, Cu, Zn). Catalysts, 2020, 10, 1444.	3.5	3
117	Lubrication effectiveness of composite lubricants during P/M electrostatic die wall lubrication and warm compaction. International Journal of Minerals, Metallurgy, and Materials, 2006, 13, 528-531.	0.2	2
118	Effect of inner oxidant on self-propagating high-temperature synthesis of MnZn-ferrite powder. Rare Metals, 2006, 25, 553-556.	7.1	1
119	Effects of heat treatment on the properties of powder injection molded AlN ceramics. Rare Metals, 2008, 27, 70-73.	7.1	1
120	Adaptive nanolaminate coating by atomic layer deposition. Thin Solid Films, 2019, 692, 137631.	1.8	1
121	High-Entropy Ceramics. , 2020, , .		1
122	Porous Ceramics for Energy Applications. , 2021, , 380-392.		0
123	Graphene Networks: Porous Strontium Chloride Scaffolded by Graphene Networks as Ammonia Carriers (Adv. Funct. Mater. 30/2021). Advanced Functional Materials, 2021, 31, 2170220.	14.9	Ο